Geographic variation in the skulls of the horseshoe bats, Rhinolophus simulator and R. cf. simulator: determining the relative contributions of adaptation and drift using geometric morphometrics.

Gregory Mutumi[1], David Jacobs[2], and Lunga Bam[3]

[1]University of California System
[2]University of Cape Town
[3]South Africa Nuclear Energy Corporation

November 25, 2020

Abstract

The relative contributions of adaptation and drift to morphological diversification of the crania of echolocating mammals was investigated using two horseshoe bat species, Rhinolophus simulator and R. cf. simulator as test cases. We used 3D geometric morphometrics to compare the shapes of skulls of the two lineages collected at various localities in southern Africa. Shape variation was predominantly attributed to selective forces; the between population variance (B) was not proportional to the within population variance (W). Modularity was evident in the crania of R. simulator but absent in the crania of R. cf. simulator and the mandibles of both species. The skulls of the two lineages thus appeared to be under different selection pressures, despite the overlap in their distributions. Selection acted mainly on the nasal dome region of R. cf. simulator whereas selection acted more on the cranium and mandibles than on the nasal domes of R. simulator. Probably the relatively higher echolocation frequencies used by R. cf. simulator, the shape of the nasal dome, which acts as a frequency dependent acoustic horn, is more crucial than in R. simulator, allowing maximization of the intensity of the emitted calls and resulting in comparable detection distances. In contrast, selection pressure is probably more pronounced on the mandibles and cranium of R. simulator to compensate for the loss in bite force because of its elongated rostrum. The predominance of selection probably reflects the stringent association between environment and the optimal functioning of phenotypic characters associated with echolocation and feeding in bats.

Geographic variation in the skulls of the horseshoe bats, *Rhinolophus simulator* and *R. cf. simulator*: determining the relative contributions of adaptation and drift using geometric morphometrics.

Gregory L Mutumi[1&2*], David S Jacobs[1*], and Lunga Bam[3]

[1] Animal Evolution and Systematics Group (AES), Department of Biological Sciences, University of Cape Town, Cape Town 7701, South Africa

[2] Life and Environmental Sciences Department, University of California–Merced, Merced, USA

[3] Radiation Science Department, South Africa Nuclear Energy Corporation, Pretoria, South Africa

Running Head: Selection and drift of bats

Key Words

Diversification, geometric morphometrics, Lande's model, micro-evolutionary forces, modularity, neutral evolution, speciation,

*** Corresponding Author**

E-mail:*gmutumi@gmail.com (GLM)*

E-mail:

david.jacobs@uct.ac.za (DSJ)

Abstract

The relative contributions of adaptation and drift to morphological diversification of the crania of echolocating mammals was investigated using two horseshoe bat species, *Rhinolophus simulator* and*R. cf. simulator* as test cases. We used 3D geometric morphometrics to compare the shapes of skulls of the two lineages collected at various localities in southern Africa. Shape variation was predominantly attributed to selective forces; the between population variance (B) was not proportional to the within population variance (W). Modularity was evident in the crania of *R. simulator* but absent in the crania of *R. cf. simulator* and the mandibles of both species. The skulls of the two lineages thus appeared to be under different selection pressures, despite the overlap in their distributions. Selection acted mainly on the nasal dome region of *R. cf. simulator* whereas selection acted more on the cranium and mandibles than on the nasal domes of *R. simulator* . Probably the relatively higher echolocation frequencies used by *R. cf. simulator* , the shape of the nasal dome, which acts as a frequency dependent acoustic horn, is more crucial than in *R. simulator* , allowing maximization of the intensity of the emitted calls and resulting in comparable detection distances. In contrast, selection pressure is probably more pronounced on the mandibles and cranium of*R. simulator* to compensate for the loss in bite force because of its elongated rostrum. The predominance of selection probably reflects the stringent association between environment and the optimal functioning of phenotypic characters associated with echolocation and feeding in bats.

Introduction

Understanding the relative contributions of drift and adaptation to organismal diversification is fundamental to studies of evolutionary ecology. To avoid overestimation of selection, drift should always be explicitly accounted for (Betti*et al.* , 2010). However, quantifying the relative contributions of these processes to phenotypic diversification is challenging because distinguishing the two processes and identifying their impacts on diversity is difficult (Brandon & Carson, 1996; Millstein, 2002, 2008; Brandon, 2005). Fortunately, there has been some progress in this regard (Millstein, 2008). Adaptation is deterministic and results in phenotypic patterns correlated to environmental/climatic clines (Millstein, 2008). In contrast drift is neutral and results from random processes affecting the genetic composition of populations (Millstein, 2008). In many cases, drift is assumed when evidence for selection is not found (Millstein 2008). However, mathematical approaches e.g. Lande's model (Lande, 1976, 1979), that allow the quantification of the effects of drift on patterns of phenotypic variation, has made it possible to directly determine the relative importance of drift and selection to phenotypic variation.

Although the application of Lande's model to phenotypic traits that vary seasonally (e.g. body weight) or are flexible (e.g. behaviour) is theoretically possible e.g. Mutumi *et al* . (Mutumi *et al.* , 2017), application of the model to such data might lead to different results depending on when the traits are sampled. In contrast, hard tissue e.g., bony skeletons including skulls provide a more permanent record of the evolutionary processes that a species has endured over its history. Several studies have therefore suggested the use of skulls and geometric morphometrics for enquiries into the relative roles of drift and selection e.g., Evin *et al* . (Evin *et al.* , 2008).

Skulls serve functions crucial to the fitness of organisms and their diversification is likely primarily through adaptation (Santana *et al.* , 2012). The neurosensory system (brain), diet acquisition structures, olfactory system, visual system, speech and sound systems are integrated and housed in the skull. Skulls are therefore subject to diverse selection pressures imposed by the environment on these systems (Cheverud, 1982; Pedersen, 1998; Klingenberg, 2008). For example, the evolution of increased head height, prominent temporal ridge and huge jaw adductor muscles in Chamaeleonid lizards were associated with strong bite force (Herrel & Holanova, 2008). The association between skull morphology and bite force has also been demonstrated in many other vertebrates (Cleuren *et al.* , 1995; Freeman & Lemen, 2008; Curtis*et al.* , 2010; Davis *et al.* , 2010). For example, elongated snouts in some fish appear to be an adaptation which facilitates feeding through suction (Westneat, 2005). Besides dietary adaptations, other behaviours relevant to fitness have shaped the evolution of skull shape. These are grooming (Rosenberger & Strasser, 1985), fighting with conspecifics (Huyghe *et al.* , 2005), building shelters (Zuri*et al.* , 1999; Hansell, 2000; Santana & Dumont, 2011) and sensing the environment (Oelschläger, 1990; Ross & Kirk, 2007).

The role of drift was demonstrated in the evolution of human skull form and shape (Rogers Ackermann & Cheverud, 2002; Betti *et al.* , 2010) using quantitative models. Smith (Smith, 2011) showed that some parts (basicranium, temporal bone, and face) of the skull evolved neutrally whereas the mandible evolved through selection. Quantitative and population genetic methods have shown that isolation between Neanderthal and modern human populations led to cranial diversification through genetic drift rather than the commonly proposed adaptive explanations (Weaver *et al.* , 2007). Similarly, Ackermann and Cheverud (Rogers Ackermann & Cheverud, 2002; Ackermann & Cheverud, 2004) applied Lande's model (Lande, 1976, 1979) to variation in the shape and size of human and monkey skulls and found that drift played a significant role. The role of selection may thus be exaggerated if drift is not accounted for quantitatively (Smith, 2011). This is especially important because studies within the same genus have yielded conflicting results. For example, drift was proposed as the cause of phenotypic convergence and divergence in two horseshoe bats, *Rhinolophus darlingi* (Jacobs *et al.* , 2013) and *Rhinolophus monoceros*(Chen *et al.* , 2009), respectively. In contrast, selection was implicated in the divergence within two other horseshoe bat species,*Rhinolophus capensis* (Odendaal *et al.* , 2014), and *R. ferrumequinum* (Sun *et al.* , 2013). Thus, two of the four studies on horseshoe bats (genus Rhinolophus) suggest that selection is the predominant driver of diversification but the other two suggest that drift is the main factor. A rigorous test of the processes behind phenotypic diversification should therefore employ models that weigh the relative contributions of adaptation and drift to determine which is the more dominant process shaping phenotypic variation.

The evolution of skull morphology in animals that rely on acoustic signals for communication or navigation (e.g. bats, dolphins, whales, rodents and birds) is particularly interesting because it adds a whole suite of selection pressures on the skull besides those associated with diet and the other five senses (Santana & Lofgren, 2013). For example, there are prominent resonant chambers (forming the nasal dome) in the nasal region of the skulls of horseshoe bats (Rhinolophidae) which acts as an acoustic horn (Hartley & Suthers, 1988; Pedersen, 1998) allowing echolocation call frequencies to be filtered and emitted at high intensity.

Using 3-D geometric morphometrics and Lande's model we investigated the relative roles of adaptation and drift in two African horseshoe bat lineages, *Rhinolophus simulator* and *R. cf. simulator* (Dool*et al.* , 2016) that are of similar size but differ markedly in the frequency of their echolocation calls. *R. cf. simulator* was previously classified as *R. swinnyi* but genetic analyses, using six nuclear markers and an mtDNA fragment (Dool *et al.* , 2016), indicated that *R. swinnyi* to the northeast of South Africa was indistinguishable from *R. simulator* , despite marked differences in the frequency of their echolocation pulses. The frequency of echolocation pulses have a direct impact on the operational range of echolocation and is generally inversely correlated with body size in bats (Jones, 1996, 1999; Jacobs *et al.* , 2007; Jacobs & Bastian, 2018) and with the volume of the nasal dome in the Rhinolophidae (Jacobs*et al.* , 2014). *R. cf. simulator* uses higher frequency echolocation calls which are more affected by atmospheric attenuation and probably must emit its calls at greater intensity to achieve the same operational range as *R. simulator* . We therefore hypothesised that selection rather than drift should be the predominant process in the evolution of skull shape because of the vital sensory and foraging functions of the skull. We predicted: 1) significant deviation from proportionality

between the within and between population trait variance in both species (Rogers Ackermann & Cheverud, 2002); 2) modularity should be more prevalent in the crania of both species than in the mandible because of the central role of echolocation to the survival and reproduction of bats. Independence between the cranium and muzzle allows for relatively more flexible response to sensory driven selection. Additionally, the existence of modularity would indicate that the skull is under directional selection because drift and stabilizing selection are inefficient at creating modularity (Melo & Marroig, 2015).

Materials and Methods

Study sites and animals

Skulls were extracted from voucher specimens of both lineages collected in support of two other studies, Mutumi *et al* . (Mutumi *et al.* , 2016) and Dool *et al* . (Dool *et al.* , 2016). These skulls were supplemented with museum specimens of both lineages (S1 Table). The distributional ranges of the two focal species *Rhinolophus simulator* (four localities) and *R. cf. simulator* (four localities) follow a latitudinal gradient ranging from 16°S to 32°S in south eastern Africa (fig. 1 in Mutumi *et al* . (Mutumi *et al.* , 2016)). Both *R. simulator* and *R. cf. simulator* lineages have pulses dominated by a constant frequency but at different frequencies with means of 80 and 107 kHz, respectively, when at rest (see fig. S1 in Mutumi *et al.* (Mutumi *et al.* , 2016)). The two lineages occur in seven woodland types; eastern half of southern Africa, ranging from DRC in the north, through Zimbabwe and Botswana into South Africa in the south. Woodland types include the Central Zambezian Miombo woodland in DRC and Zambia, the Zambezian and Mopane woodlands, Southern Miombo woodlands, and the Eastern Zimbabwe Montane Forest-grassland Mosaic (Olson *et al.* , 2001). The southern-most populations occur within Highveld grasslands. In Botswana the sampling site occurred in an ecotone of three woodlands: Kalahari Acacia-Baekiaea, Kalahari Xeric Savannah, and Southern Africa bushveld. Botswana sites experience the driest climate and the Eastern Zimbabwe Montane Forest-grassland Mosaic, the wettest (Olson *et al.* , 2001).

The specimens were grouped according to the geographic location where they were captured (S1 Fig a and b; Table A1). These locations included north-eastern South Africa (NE), northern Zimbabwe and combined southern Zambia (NZ), Democratic Republic of Congo (DR), south-eastern South Africa (SE), southern Zimbabwe and northern South Africa combined (SZ; S1 Fig a and b; Table A1).

3-D images of each skull were captured through micro-focus X-ray tomography at the South African Nuclear Energy Corporation (NECSA, Pretoria, South Africa; (Hoffman & De Beer, 2012)) following the same procedures as in Jacobs *et al* . (Jacobs *et al.* , 2014). All images were imported into the 3-D imaging software, Avizo (version 8.0; Visualization Sciences Working Group, Merignac, France) as volume files. After creating iso-surfaces from the volume files in Avizo, files were saved in 'Stanford ply' format and opened in Meshlab (version 1.3.3, Visual Computing Lab of ISTI - CNR, Italy) for placing landmarks. Landmarks were chosen depending on their homology (common and repeatable points on all skulls for each lineage). One skull and one mandible were first tested by repeating the land-marking process 10 times to determine the precision at which landmarks could be placed. Among the tested landmarks the most precise were selected, i.e., 24 landmarks for the skull and 15 for the mandible (S2 Table). Landmarks were placed on only the right half of the skull and the right mandible to control for possible asymmetry (Jacobs *et al.* , 2014). Each landmark in the 3D space had three coordinates (x, y and z). These sets of three coordinates were used in MorphoJ (version 1.7.0_45; (Klingenberg, 2011)) to analyse shape variation in skulls and mandibles of the two lineages across different localities.

Landmark co-ordinates were analysed as follows. Firstly, a Procrustes superimposition was done on the coordinates to remove variation because of differences in orientation and scale and to standardise the landmarks in a common coordinate system (Adams *et al.* , 2004). Outliers were checked and extreme cases were double-checked against the original volume files. Where necessary the landmarks were re-inserted on the skull images. A covariance matrix was generated from the Procrustes coordinates, on which a principal components

analysis was performed to explore variation in skull shape amongst the different localities for each species. A Procrustes ANOVA (provided in MorphoJ software) was used to test the significance of the differences in skull shapes across localities and between sexes. To visualise the shape differences, a Canonical Variate analysis (CVA) was used. Shape changes in the skulls and mandibles were visualised using the wireframe outlines in MorphoJ which compares shape variations against the average skull shape along each Canonical Variate (CV) with the outlines at the extremes of each CV.

Modularity was also investigated using *a priori* hypotheses according to Klingenberg (Klingenberg, 2009). Modularity is the differential evolution of different complexes, each complex consisting of groups of traits that evolve together but relatively autonomously from other such complexes (Cheverud, 1996; Wagner, 1996; Klingenberg, 2005). Processes contributing to modularity can be genetic, developmental, functional, or environmental (Klingenberg, 2005). The mandible was divided into subsets of seven (ascending ramus) and eight (alveolar region) landmarks and the cranium was divided into subsets of 10 (basicranium) and eight (rostrum) landmarks as in Jojic *et al* . (Jojić *et al.* , 2015). The strength of association between hypothesized modules and all alternative partitions were tested by the CR – covariance ratio in R statistics according to Adams (Adams & Otárola-Castillo, 2013). The CR measures the strength of association between two blocks, i.e., the two modules identified by the covariance matrices of their landmark coordinates compared with the two hypothesised modules (Adams & Otárola-Castillo, 2013). The CR varies from 0 (completely uncorrelated data) to 1.0 (correlated). The strength of the modularity was also measured by the Z_{cr}coefficient which measures the strength of modularity in each structure – the more negative the coefficient the higher the strength of modularity.

Lande's Model

The relative contributions of drift and adaptation to the variation in skull and mandible shape was tested by applying the principles of Lande's model (Lande, 1976, 1979) in the form of the β -test (Rogers Ackermann & Cheverud, 2002), which is described in detail in Mutumi *et al* . (Mutumi *et al.* , 2017). The β -test is based on the hypothesis of a log-linear relationship between the variation of phenotypic characteristics between (B) and within (W) populations. If the slope of this relationship is not significantly different from one the null hypothesis is accepted and the observed variations in phenotypic traits can be attributed to neutral evolutionary processes (mutation and drift). Otherwise, the null hypothesis is rejected, which implies that non-neutral evolutionary processes, such as natural selection, can be inferred as the dominant driver of diversification.

Successive landmark coordinates were used to generate Euclidean distances (D) for successive pairs of landmarks using the following formula:

Where x, y and z are the 3-D landmark coordinates, the subscripts 1 and 2 denote successive positions, and D_i is the Euclidean distance for landmark i.

The resulting multivariate response matrix comprisingD_i was used to derive the within locality (W) and between locality *(B)* variances following the procedure outlined in Mutumi *et al* . (Mutumi *et al.* , 2017). Briefly, the D_i response matrix was fitted using MANOVA with localities and sex as the categorical predictors to generate a variance/covariance (V/CV) matrix for each species. A measure of the within- population variance W was then obtained in the form of eigenvalues derived from principal component analysis (PCA) on the V/CV matrix. The between population variation B was estimated through multiplication of the matrix of PCA-derived eigenvectors with the matrix of D_i means of each locality. We then regressed the log-transformed within variance against the log-transformed between variance and carried out regression t-tests to test the hypothesis that there was no significant difference between the regression slope and one as a function of:

Where β_0 is the intercept term and ϵ is the error (see Mutumi *et al* . (Mutumi *et al.* , 2017)).

Results

A total of 56 skulls and 50 mandibles of *R. simulator* and 19 skulls and 14 mandibles of *R. cf. simulator* were analysed. Procrustes ANOVA tests did not find significant differences between sexes in both species (both in size and shape of skulls and mandibles). For *R. simulator* skull size, $F_{1;\,54} = 2.19$, $p = 0.14$; skull shape, $F_{65;\,3510} = 1.01$, $p = 0.46$; mandibles size, $F_{1;\,49} = 4.77$, $p = 0.03$; mandible shape $F_{38;\,1862} = 2.47$; $p < 0.0001$. For *R. cf. simulator* skull size,$F_{1;\,17} = 1.25$, $p = 0.28$; skull shape,$F_{65;\,1105} = 0.93$, $p = 0.64$; mandible size,$F_{1;\,12} = 3.97$,; $p = 0.07$, mandible shape,$F_{38;\,456} = 0.79$, $p = 0.81$. Sexes were therefore pooled for all analyses, balancing the number of males and females for *R. simulator* mandibles.

There was variation in the shape of skulls across different localities within each lineage (*R. simulator* : $F_{195;\,3445} = 2.22$; $p < 0.001$, *R. cf. simulator* :$F_{130;\,1040} = 2.37$; $p < 0.001$) but not in size (*R. simulator* skulls: $F_{3;\,53} = 0.15$, $p = 0.93$; *R. cf. simulator* skulls:$F_{2;\,16} = 2.57$; $p = 0.11$). The mandibles of*R. cf. simulator* differed in shape across localities ($F_{76;\,418} = 1.52$; $p < 0.01$) but not size (*R. cf. simulator* mandibles: $F_{2;\,11} = 1.68$; $p = 0.23$). Those of *R. simulator* were not different in both shape ($F_{114;\,1786} = 0.38$;$p = 0.15$) and size ($F_{3;\,47} = 0.17$;$p = 0.91$).

Skulls

For *R. simulator* , the first two canonical variates of the canonical variate analysis (CVA) of shape variation amongst the localities of *R. simulator* explained a total of 90% of the variation (Fig. 1). The wireframe graphs (Fig. 1) show that the first canonical variate (CV1) was associated with changes in the palate, zygomatic arch, cranium and cochlea structure (66% of the variation). Skulls from the NZ locality fell at the positive end of CV1 and appeared to have a wider zygomatic arch, broader cochlea and longer palates relative to the average. Conversely, skulls from the SE locality fell at the negative end of CV1 and had a reduced zygomatic arch, a narrower cochlea and shorter palates relative to the average. Two localities (NE and SZ) fell within the intermediate zone of the CV prescribed shape space, implying that it had a shape close to the average. CV2 was mostly associated with the anterior medial swelling (24% of the variation; Fig. 1). The SZ locality fell at the positive end of CV2 and had an outline implying increased volume of the nasal dome relative to the average. Skulls from two localities (NE and NZ) fell at the negative end of CV2 indicating that they had a smaller anterior medial swellings than the average, and skulls from one locality (SE) were positioned intermediately along CV2 indicating that it had an anterior medial swelling close to the average. CV3 (S2 Fig) explained 10% of the variation and was associated with changes in the zygomatic arch and palate. Skulls from NZ and SE were on the negative end of CV3 suggesting that they had broader zygomatic arches, and longer palates relative to the average shape and the position of SZ and NE along CV3 indicated that these skulls had narrower zygomatic arches and shorter palates relative to the average shape (S2 Fig).

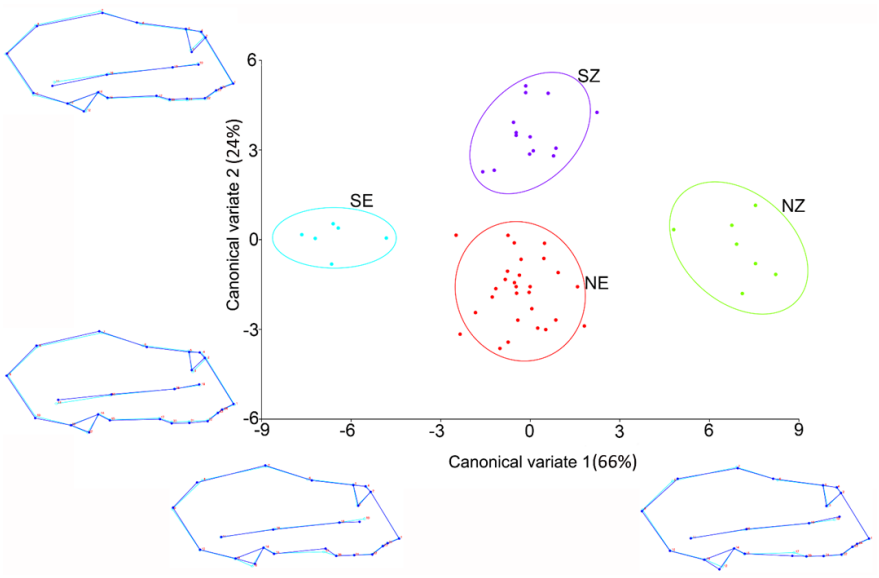

Figure 1: The first two canonical variates of the canonical variate analysis (CV1 and CV2) of skull shape variation amongst localities of *R. simulator* . Light blue outline represents the average shape; dark blue outline shows the deviation of shape of the skull from the average. Locality abbreviations: NZ = northern Zimbabwe, SZ = southern Zimbabwe and parts of northern South Africa and south of Botswana, NE = north-eastern South Africa, SE = south-eastern South Africa, and DR = Democratic republic of Congo.

For *R. cf. simulator* , the first two canonical variates of CVA of shape variation amongst localities explained 100% of the variation (Fig. 2). CV1 was associated with changes in the caudal region and anterior medial swelling of the skull, as shown by the wireframe graphs (77% of the variation; Fig. 2). The NZ locality fell at the positive end of CV1 and appeared to have a smaller and more anteriorly positioned anterior medial swelling and a narrower and more shortened cranium than the average shape. Conversely, DR locality fell at the negative end of CV1 and had a larger more posterior nasal dome, a broader and longer cranium relative to the average. One locality (NE) fell within the intermediate shape zone. CV2 was associated with the cochlea and caudal dimensions (Fig. 2). All localities seemed to group on the average shape space for CV2 which accounted for 23% of the variation. CV3 could not be derived from the *R. cf. simulator* data set because of the small sample size.

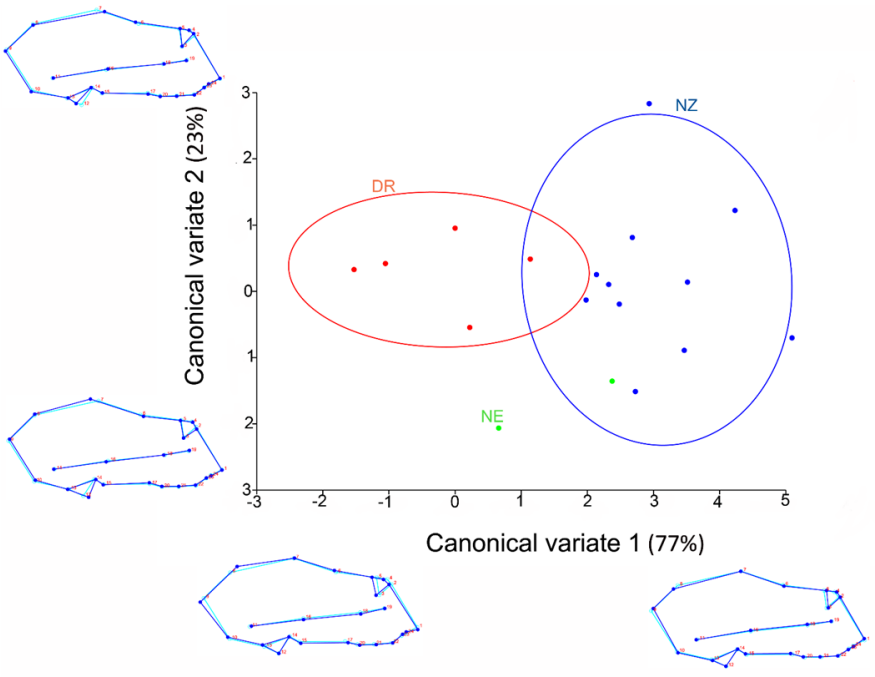

Figure 2: The first two canonical variates of the canonical variate analysis (CV1 and 2) of skull shape variation amongst localities of *R. cf. simulator* . Light blue outline represents the average shape; Dark blue outline shows the variation of shape of skulls from the average. Locality abbreviations are the same as in Fig. 1.

Mandibles

For *R. simulator* , the first two canonical variates of the canonical variate analysis (CVA) of shape variation amongst the localities of *R. simulator* explained 95% of the variation (Fig. 3). CV1 was only associated with the thickness of the alveolar bone, all the other dimensions seemed consistent with the average shape (60% of the variation; Fig. 3). The NE locality fell at the positive end of CV1 and had an outline implying a thicker alveolar bone relative to the average. SZ, NZ and SE fell at the negative end of CV1 and appeared to have a thinner alveolar bone relative to the average (Fig. 3). CV2 was associated with changes in height of the ascending ramus and the thickness of the alveolar bone (35% of the variation; Fig. 3). The SE and NZ locality fell at the positive end of CV2 and appeared to have a shorter ascending ramus and a thicker alveolar bone relative to the average. Conversely, SZ locality fell at the negative end of CV2 and had a taller ascending ramus and a thinner alveolar bone relative to the average. NE fell within the intermediate shape zone (Fig. 3). CV3 (5% of the variation; S3 Fig) did not show much variation in the mandible, all the localities grouped on the average shape space except the NZ locality which seemed to have a slightly thinner alveolar bone (at the anterior region of the bone).

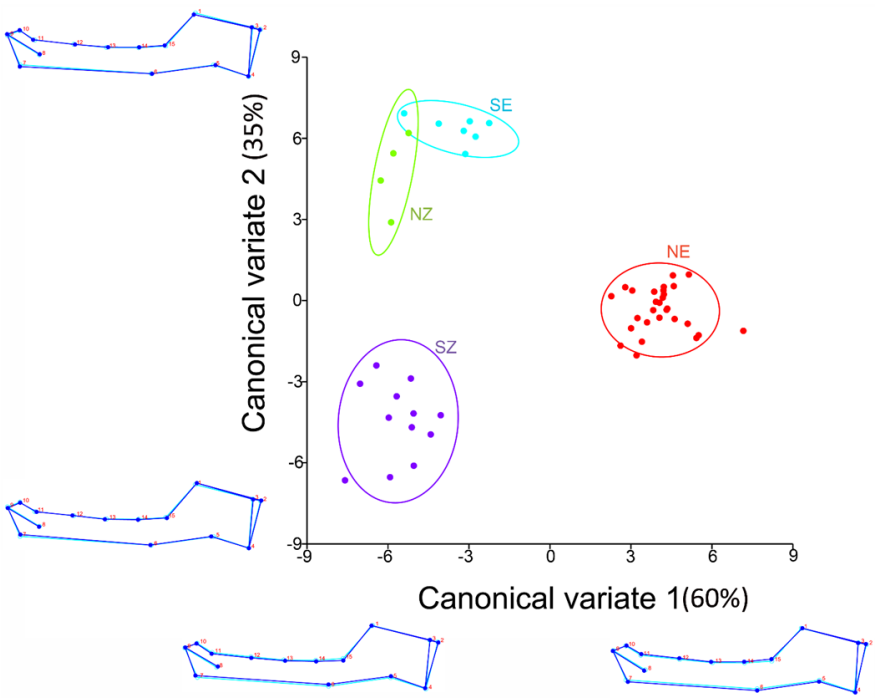

Figure 3: The first two canonical variates of the canonical variate analysis (CV1 and 2) of mandible shape variation amongst localities of *R. simulator* . Light blue outline represents the average shape; Dark blue outline shows the deviation of shape of mandibles from the average. Locality abbreviations are the same as in Fig. 1.

.

For *R. cf. simulator* , the first two canonical variates of the CVA of shape variation amongst the localities explained 100% of the variation (Fig. 4). CV1 was associated with changes in the total length of the mandible, thickness of the ascending ramus and the thickness of the alveolar bone as shown by the wireframe graphs (85% of the variation; Fig. 4). The NZ localities fell at the positive end of CV1 and appeared to have a shorter total length of mandible, a thinner ascending ramus, and a thinner alveolar bone than the average shape. Conversely, DR and NE localities fell at the negative end of CV1 and had a longer total length of mandible and thicker alveolar bone relative to the average. CV2 was associated with ascending ramus dimensions and position of the incisor teeth (15% of the variation; Fig. 4). The DR locality was at the positive end of CV2 and had an outline implying a shorter ascending ramus and more posterior incisors relative to the average. NZ was at the negative end of CV2 suggesting a slightly longer ascending ramus and slightly posterior incisors than the average shape (Fig. 4).

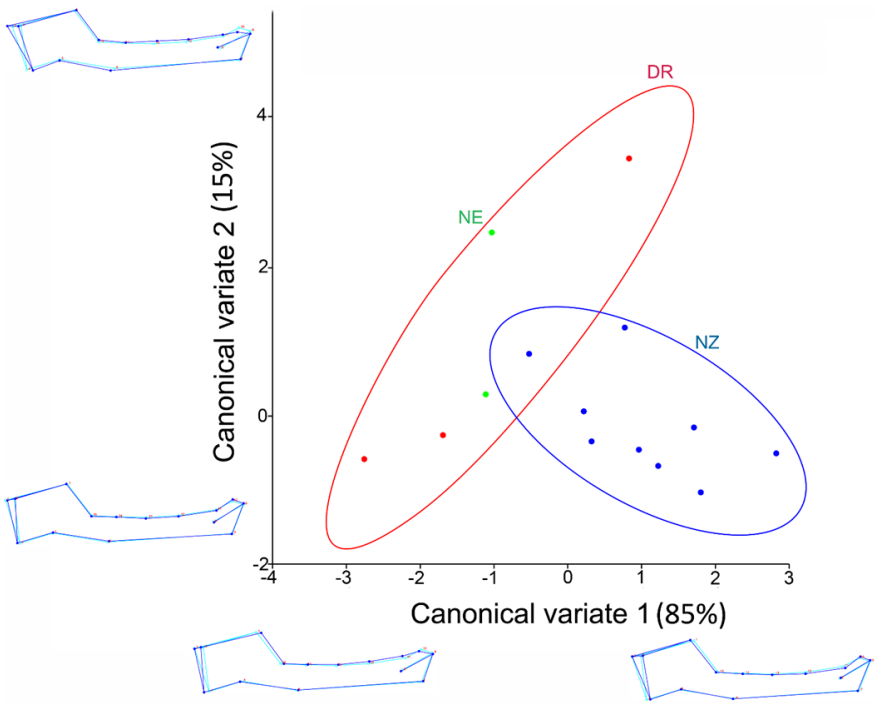

Figure 4: The first two canonical variates of the canonical variate analysis (CV1 and 2) of mandible shape variation amongst localities of *R. cf. simulator* . Light blue outline represents the average shape; Dark blue outline shows the variation of shape of mandible from the average shape. Locality abbreviations are the same as in Fig. 1.

Modularity

The caudal and rostral regions of *Rhinolophus simulator* skulls evolved as separate modules (CR = 0.452, Z_{cr} = -2.494P = 0.004). Contrarily the mandible of *R. simulator*(ascending ramus and alveolar bone) did not show any modularity (CR = 1.106, Z_{cr} = 0.887, P = 0.836). Both skulls (CR = 0.821, Z_{cr} = -1.276, P = 0.092) and mandibles (CR = 0.859, Z_{cr} = -1.168, P = 0.09) of *R. cf. simulator* did not show strong modularity between the partitions analysed.

Lande's Model

All regression slopes describing the relationship between Ln (W) and Ln *(B)* differed significantly from one (Table 1) and showed no consistency in the direction of slopes (S4 Fig). All the graphs were positive except the *R. cf. simulator* mandibles which showed a negative trend (S4 Fig). This indicated that none of the tests were consistent with drift and that the shape and size of skulls and mandibles of *R. simulator* and *R. cf. simulator* may have evolved predominantly through selection across different populations. The selective pressure responsible for the variation in skull shapes and sizes appeared to be stabilising because there was less variation between localities than within localities for both species. It is possible that strong stabilising selection was acting on*R. cf. simulator* mandibles because these show the strongest and negative deviation from the slope predicted for drift. The limited sample size did not permit analyses by exclusion as in Mutumi *et al* . (Mutumi *et al.* , 2017). This means that site specific signals of drift could not be detected by the current analysis.

Table 1. Results from Lande's model on the 3D coordinate landmarks of skulls and mandibles of *Rhinolophus*

simulator and*R. cf. simulator* from different localities within southern Africa.

	Slope b	S.E.	p (β [;] 1)	Consistent with Drift
R. simulator skulls	0.408	0.093	$p < 0.001$	No
R. cf. simulator skulls	0.285	0.160	$p < 0.001$	No
R. simulator mandibles	0.150	0.067	$p < 0.001$	No
R. cf. simulator mandibles	-0.192	0.165	$p < 0.001$	No

Slope b : estimation of regression slope, along with the standard error (S.E.) and p (β [;] 1) p -value for the null hypothesis of $b = 1$.

Discussion

The relationship between the within and between group variance did not comply with the predictions of the model for drift. As predicted, geographic variation in the skulls and mandibles of both lineages was thus likely the result of selection, in accordance with our first prediction. Modularity was only supported in *R. simulator* skulls, the cranium and muzzle evolving as separate and integrated units. Contrary to our second prediction, the mandible of *R. simulator*and both the skull and mandible of *R. cf. simulator* , did not show modularity. Thus the two closely related lineages (Dool *et al.* , 2016) showed contrasting results with respect to modularity. We also found evidence consistent with our hypothesis that more prominent variation in shape were seen in the nasal dome in *R. cf. simulator* than in *R. simulator* . Thus Lande's model indicates that selection rather than drift has shaped the skulls of these two lineages. The results on modularity (see reference 43) suggest that the selection responsible for the diversification of *R. simulator* is predominantly directional (in the skull) and stabilising in the mandibles, whereas in *R. cf. simulator* , is mainly stabilising for both the skull and the mandible.

To some extent, these results contrast with previous findings on the relative contributions of drift and adaptation based on Lande's model which identified signals of drift in some instances (Marroig & Cheverud, 2004; Weaver *et al.* , 2007). Mutumi *et al* . (Mutumi *et al.* , 2017) report signals for drift but their study was based on a broader range of phenotypic features including flight, size and echolocation parameters. Perhaps the fact that the skull incorporates several functions (e.g., feeding and echolocation) crucial to fitness causes it to be under severe selection pressure that could eliminate or obscure any drift that might have occurred. The head is under the influence of multiple selective pressures because it houses the structures used for a variety of crucial survival and reproduction functions, particularly echolocation. Both lineages appear to have experienced selection pressure associated with echolocation, a key survival trait. Echolocation is a sophisticated sense that varies strongly with the task at hand and environmental conditions (Schnitzler*et al.* , 2003; Jakobsen *et al.* , 2013; Luo *et al.* , 2014).

It surprising that modularity was present only *R. simulator* and not in *R. cf. simulator* because modularity has been reported across 22 African and Asian species of rhinolophids (Santana & Lofgren, 2013). However, stabilizing selection is thought to mitigate against the evolution of modularity (Melo & Marroig, 2015). The absence of modularity in *R. cf. simulator* may be a consequence of stabilizing selection to retain the adaptive complex between flight, body size and echolocation. In this respect the evolution of *R. cf. simulator* is similar to Phyllostomidae which is tightly integrated and probably evolved under the constraint of preserving adaptive complexes (Hedrick *et al.* , 2019). Body size, wing loading and echolocation frequency in bats are associated allometrically and are indicative of an adaptive complex (Jones, 1999; Jacobs *et al.* , 2007; Jacobs & Bastian, 2018). With respect to these allometric relationships *R. cf. simulator* is an average rhinolophid. Its echolocation frequency and wing loading fall within the allometric relationships of the genus (Jacobs *et al.* , 2007; Jacobs & Bastian, 2018).

In contrast to *R. cf. simulator* there was evidence of modularity in *R. simulator* suggesting that its skull was under directional selection (48). Unlike *R. cf. simulator* , the adaptive complex between echolocation frequency and body size is absent. Although its wing loading scaled allometrically with body size, *R. simulator*echolocated at a lower frequency for its body size (Jacobs *et al.* , 2007; Jacobs & Bastian, 2018). Furthermore, it also had lower echolocation frequencies than would be predicted by the volume of its nasal capsules (Jacobs *et al.* , 2014). This suggests directional selection for lower frequency echolocation, possibly to increase the operational range of its echolocation, reflected in the phenotype of the skull associated with echolocation. Lower frequency sound undergoes less atmospheric attenuation than high frequency sound (Lawrence & Simmons, 1982) and, all else being, the echolocation of *R. simulator*should therefore have longer operational ranges than *R. cf. simulator* , unless it emits echolocation pulse at lower intensities. Currently the intensities at which these two lineages emit their echolocation pulses are unknown. If the same, the fact that *R. simulator* and *R. cf. simulator* were sometimes caught at the same locality and from the same cave, suggests that their use of different echolocation frequency with consequent differences in the operational range of their echolocation pulses, may be a means of partitioning their foraging habitat, if not their diet. In both lineages, the mandible evolved as one complete module (ascending ramus and alveolar bone) contrary to the mandibular modularity found in *R. ferrumequinum*(Jojić *et al.* , 2015). The mandible has therefore possibly evolved under constraint and might be following a line of least evolutionary resistance as in the phyllostomids (Hedrick *et al.* , 2019). The mandible variations across localities did not show any difference between the two species except the variations on the position of the incisors that were seen in *R. cf. simulator* but not in *R. simulator* . The similarities between the mandibles signifying close similarities in diet between the two species.

The marked influence of echolocation on the skull of both *R. simulator* and *R. cf. simulator* is also reflected in variations in the shapes of cochlea in both species. This suggests that selection has acted strongly on both sound production and perception functions in the two lineages. Variations in the morphology of the cochlea are related to variations in perceptions of sound, particularly in rhinolophids (Davies *et al.* , 2013). For example, in rhinolophids the cochlear basal turn is expanded, more so than in other bats (Davies*et al.* , 2013), probably because of the well-developed auditory fovea in this taxon allowing the Doppler shift compensation upon which high duty cycle echolocation is based (Neuweiler, 2003). The frequency of echolocation pulses in rhinolophids are also negatively associated with the length of the basilar membrane length and positively associated with the number of cochlear turns (Davies *et al.* , 2013). These relationships suggest that the cochlea of these bats probably track the acoustic properties of the habitats they occupy, hence the geographic variation reported here in both echolocation frequency and cochlea morphology. The finer details of the mechanistic association between cochlea morphology and echolocation parameters still need to be elucidated (Davies *et al.* , 2013).

The differences in the selection pressures experienced by the two lineages are remarkable given the genetic similarity of the two lineages at least in the genetic markers considered by Dool et al. (Dool *et al.* , 2016). The two lineages were indistinguishable across 6 nuclear introns and one mitochondrial fragment. It has been suggested that *R. cf. simulator* is possibly a cryptic lineage, sister to *R. simulator* (Dool *et al.* , 2016), a view supported by the differences in the evolution of skulls reported here. However, the two lineages occur at the same sites and sometimes in the same caves and there is some evidence of hybridization between the two lineages. This raises the question of how they can maintain such divergent and non-overlapping echolocation frequencies. The answer to this question requires evolutionary development studies to identify the loci which code for echolocation frequency (e.g., Sun et al (Sun *et al.* , 2020)) and how these loci are assorted during gamete formation.

Conflict of Interest

The authors declare no competing interests

Ethical Statement

Capture, handling, and voucher collection complied with the guidelines recommended by the American

Society of Mammalogists (Gannon and Sikes, 2007), and small mammal sampling guidelines compiled by Aegerter and Heritage (2005) and Kunz and Parsons (2009); and were approved by the Science Faculty Animal Ethics Committee at the University of Cape Town (Clearance Number 2013/2011/V6/DJ). All workers handling bats were vaccinated for rabies and were required to use protective gloves when handling bats and samples.

Authors' Contributions

GLM, and DSJ conceived and designed the study. GLM, DSJ and LB carried out the fieldwork. GLM conducted the ecological analyses with input from DSJ. GLM, and DSJ, and LB contributed to the writing of the manuscript and read and approved the final manuscript.

Acknowledgements

We would like thank NECSA (South African Nuclear Energy Corporation SOC Limited) and specifically the RADTOM-team (Kobus Hoffman & Frikkie de Beer) for dedication and time invested for the free scanning of the skulls and the Department of Science & Technology and the National Research Foundation for financing the NIKON micro-focus X-ray tomography system. For help with R scripts, we would like to thank Henning Winker. This project was funded by research grants to DSJ from the South African Research Chair Initiative of the Department of Science and Technology and administered by the National Research Foundation of South Africa (GUN 64798) and the University Research Committee of the University of Cape Town.

Data Availability

All specimens are deposited in publicly accessible collections (Table S1). Sampling locations, morphological data, and scripts will be stored in a publicly accessible repository such as Dryad.

References

Ackermann, R.R. & Cheverud, J.M. 2004. Morphological integration in primate evolution. *Phenotypic Integr. Stud. Ecol. Evol. complex phenotypes* **302** : 319. Págs.

Adams, D.C. & Otárola-Castillo, E. 2013. Geomorph: An r package for the collection and analysis of geometric morphometric shape data.*Methods Ecol. Evol.* **4** : 393–399. Wiley Online Library.

Adams, D.C., Rohlf, F.J. & Slice, D.E. 2004. Geometric morphometrics: ten years of progress following the 'revolution.' *Ital. J. Zool.***71** : 5–16. Taylor & Francis.

Betti, L., Balloux, F., Hanihara, T. & Manica, A. 2010. The relative role of drift and selection in shaping the human skull. *Am. J. Phys. Anthropol. Off. Publ. Am. Assoc. Phys. Anthropol.* **141** : 76–82. Wiley Online Library.

Brandon, R.N. 2005. The difference between selection and drift: A reply to Millstein. *Biol. Philos.* **20** : 153–170. Springer.

Brandon, R.N. & Carson, S. 1996. The indeterministic character of evolutionary theory: no" no hidden variables proof" but no room for determinism either. *Philos. Sci.* **63** : 315–337. University of Chicago Press.

Chen, S.-F., Jones, G. & Rossiter, S.J. 2009. Determinants of echolocation call frequency variation in the Formosan lesser horseshoe bat (Rhinolophus monoceros). *Proc. R. Soc. B Biol. Sci.***276** : 3901–3909. The Royal Society.

Cheverud, J.M. 1996. Quantitative genetic analysis of cranial morphology in the cotton-top (Saguinus oedipus) and saddle-back (S. fuscicollis) tamarins. *J. Evol. Biol.* **9** : 5–42. Wiley Online Library.

Cheverud, J.M. 1982. Relationships among ontogenetic, static, and evolutionary allometry. *Am. J. Phys. Anthropol.* **59** : 139–149. Wiley Online Library.

Cleuren, J., Aerts, P. & Vree, F. de. 1995. Bite and joint force analysis in Caiman crocodilius. *Belgian J. Zool.*

Curtis, N., Jones, M.E.H., Lappin, A.K., O'Higgins, P., Evans, S.E. & Fagan, M.J. 2010. Comparison between in vivo and theoretical bite performance: using multi-body modelling to predict muscle and bite forces in a reptile skull. *J. Biomech.* **43** : 2804–2809. Elsevier.

Davies, K.T.J., Bates, P.J.J., Maryanto, I., Cotton, J.A. & Rossiter, S.J. 2013. The Evolution of Bat Vestibular Systems in the Face of Potential Antagonistic Selection Pressures for Flight and Echolocation. *PLoS One* **8** : 8–10.

Davis, J.L., Santana, S.E., Dumont, E.R. & Grosse, I.R. 2010. Predicting bite force in mammals: two-dimensional versus three-dimensional lever models. *J. Exp. Biol.* **213** : 1844–1851. The Company of Biologists Ltd.

Dool, S.E., Puechmaille, S.J., Foley, N.M., Allegrini, B., Bastian, A., Mutumi, G.L., *et al.* 2016. Nuclear introns outperform mitochondrial DNA in inter-specific phylogenetic reconstruction: Lessons from horseshoe bats (Rhinolophidae: Chiroptera). *Mol. Phylogenet. Evol.* **97** .

Evin, A., Baylac, M., Ruedi, M., Mucedda, M. & Pons, J.-M. 2008. Taxonomy, skull diversity and evolution in a species complex of Myotis (Chiroptera: Vespertilionidae): a geometric morphometric appraisal. *Biol. J. Linn. Soc.* **95** : 529–538. Oxford University Press.

Freeman, P.W. & Lemen, C.A. 2008. Measuring bite force in small mammals with a piezo-resistive sensor. *J. Mammal.* **89** : 513–517. American Society of Mammalogists.

Hansell, M. 2000. *Bird nests and construction behaviour* . Cambridge University Press.

Hartley, D.J. & Suthers, R.A. 1988. The acoustics of the vocal tract in the horseshoe bat, R hinolophushildebrandt i. *J. Acoust. Soc. Am.***84** : 1201–1213. Acoustical Society of America.

Hedrick, B.P., Mutumi, G.L., Munteanu, V.D., Sadier, A., Davies, K.T.J., Rossiter, S.J., *et al.* 2019. Morphological Diversification under High Integration in a Hyper Diverse Mammal Clade. *J. Mamm. Evol.*1–13. Springer.

Herrel, A. & Holanova, V. 2008. Cranial morphology and bite force in Chamaeleolis lizards–adaptations to molluscivory? *Zoology***111** : 467–475. Elsevier.

Hoffman, J.W. & De Beer, F.C. 2012. Characteristics of the micro-focus X-ray tomography facility (MIXRAD) at Necsa in South Africa. In:*18th World Conference on Nondestructive Testing* , pp. 16–20.

Huyghe, K., Vanhooydonck, B., Scheers, H., Molina-Borja, M. & Van Damme, R. 2005. Morphology, performance and fighting capacity in male lizards, Gallotia galloti. *Funct. Ecol.* 800–807. JSTOR.

Jacobs, D.S., Babiker, H., Bastian, A., Kearney, T., van Eeden, R. & Bishop, J.M. 2013. Phenotypic convergence in genetically distinct lineages of a Rhinolophus species complex (Mammalia, Chiroptera). *PLoS One* **8** : e82614. Public Library of Science.

Jacobs, D.S., Barclay, R.M.R. & Walker, M.H. 2007. The allometry of echolocation call frequencies of insectivorous bats: why do some species deviate from the pattern? *Oecologia* **152** : 583–594. Springer.

Jacobs, D.S. & Bastian, A. 2018. High duty cycle echolocation may constrain the evolution of diversity within horseshoe bats (family: Rhinolophidae). *Diversity* **10** : 85. Multidisciplinary Digital Publishing Institute.

Jacobs, D.S., Bastian, A. & Bam, L. 2014. The influence of feeding on the evolution of sensory signals: a comparative test of an evolutionary trade-off between masticatory and sensory functions of skulls in southern African Horseshoe bats (Rhinolophidae). *J. Evol. Biol.***27** : 2829–2840. Wiley Online Library.

Jakobsen, L., Brinkløv, S. & Surlykke, A. 2013. Intensity and directionality of bat echolocation signals. *Front. Physiol.***4** : 89. Frontiers.

Jojić, V., Budinski, I., Blagojević, J. & Vujošević, M. 2015. Mandibular and cranial modularity in the greater horseshoe bat Rhinolophus ferrumequinum (Chiroptera: Rhinolophidae). *Hystrix***26** .

Jones, G. 1996. Does echolocation constrain the evolution of body size in bats? In: *Symposia of the Zoological Society of London* , pp. 111–128.

Jones, G. 1999. Scaling of echolocation call parameters in bats.*J. Exp. Biol.* **202** : 3359–3367. The Company of Biologists Ltd.

Klingenberg, C.P. 2005. Developmental constraints, modules, and evolvability. In: *Variation* , pp. 219–247. Elsevier.

Klingenberg, C.P. 2011. MorphoJ: an integrated software package for geometric morphometrics. *Mol. Ecol. Resour.* **11** : 353–357. Wiley Online Library.

Klingenberg, C.P. 2008. Morphological integration and developmental modularity. *Annu. Rev. Ecol. Evol. Syst.* **39** : 115–132. Annual Reviews.

Klingenberg, C.P. 2009. Morphometric integration and modularity in configurations of landmarks: Tools for evaluating a priori hypotheses.*Evol. Dev.* **11** : 405–421.

Lande, R. 1976. Natural selection and random genetic drift in phenotypic evolution. *Evolution (N. Y).* 314–334. JSTOR.

Lande, R. 1979. Quantitative genetic analysis of multivariate evolution, applied to brain: body size allometry. *Evolution (N. Y).*402–416. JSTOR.

Lawrence, B.D. & Simmons, J.A. 1982. Measurements of atmospheric attenuation at ultrasonic frequencies and the significance for echolocation by bats. *J. Acoust. Soc. Am.* **71** : 585–590. Acoustical Society of America.

Luo, J., Koselj, K., Zseb\Hok, S., Siemers, B.M. & Goerlitz, H.R. 2014. Global warming alters sound transmission: differential impact on the prey detection ability of echolocating bats.*J. R. Soc. Interface* **11** : 20130961. The Royal Society.

Marroig, G. & Cheverud, J.M. 2004. Did natural selection or genetic drift produce the cranial diversification of neotropical monkeys?*Am. Nat.* **163** : 417–428. The University of Chicago Press.

Melo, D. & Marroig, G. 2015. Directional selection can drive the evolution of modularity in complex traits. *Proc. Natl. Acad. Sci.***112** : 470–475. National Acad Sciences.

Millstein, R.L. 2002. Are random drift and natural selection conceptually distinct? *Biol. Philos.* **17** : 33–53. Springer.

Millstein, R.L. 2008. Distinguishing drift and selection empirically:"the great snail debate" of the 1950s. *J. Hist. Biol.* **41** : 339–367. Springer.

Mutumi, G.L., Jacobs, D.S. & Winker, H. 2016. Sensory drive mediated by climatic gradients partially explains divergence in acoustic signals in two horseshoe bat species, rhinolophus swinnyi and rhinolophus simulator. *PLoS One* **11** .

Mutumi, G.L., Jacobs, D.S. & Winker, H. 2017. The relative contribution of drift and selection to phenotypic divergence: A test case using the horseshoe bats Rhinolophus simulator and Rhinolophus swinnyi.*Ecol. Evol.* **7** .

Neuweiler, G. 2003. Evolutionary aspects of bat echolocation. *J. Comp. Physiol. A* **189** : 245–256. Springer.

Odendaal, L.J., Jacobs, D.S. & Bishop, J.M. 2014. Sensory trait variation in an echolocating bat suggests roles for both selection and plasticity. *BMC Evol. Biol.* **14** : 60. Springer.

Oelschläger, H.A. 1990. Evolutionary morphology and acoustics in the dolphin skull. In: *Sensory abilities of cetaceans* , pp. 137–162. Springer.

Olson, D.M., Dinerstein, E., Wikramanayake, E.D., Burgess, N.D., Powell, G.V.N., Underwood, E.C., *et al.* 2001. Terrestrial Ecoregions of the World: A New Map of Life on EarthA new global map of terrestrial ecoregions provides an innovative tool for conserving biodiversity.*Bioscience* **51** : 933–938. Oxford University Press.

Pedersen, S.C. 1998. Morphometric analysis of the chiropteran skull with regard to mode of echolocation. *J. Mammal.* **79** : 91–103. American Society of Mammalogists 810 East 10th Street, PO Box 1897, Lawrence˜....

Rogers Ackermann, R. & Cheverud, J.M. 2002. Discerning evolutionary processes in patterns of tamarin (genus Saguinus) craniofacial variation. *Am. J. Phys. Anthropol. Off. Publ. Am. Assoc. Phys. Anthropol.* **117** : 260–271. Wiley Online Library.

Rosenberger, A.L. & Strasser, E. 1985. Toothcomb origins: support for the grooming hypothesis. *Primates* **26** : 73–84. Springer.

Ross, C.F. & Kirk, E.C. 2007. Evolution of eye size and shape in primates. *J. Hum. Evol.* **52** : 294–313. Elsevier.

Santana, S.E. & Dumont, E.R. 2011. Do roost-excavating bats have stronger skulls? *Biol. J. Linn. Soc.* **102** : 1–10. Oxford University Press.

Santana, S.E., Grosse, I.R. & Dumont, E.R. 2012. Dietary hardness, loading behavior, and the evolution of skull form in bats.*Evolution (N. Y).* **66** : 2587–2598. Wiley Online Library.

Santana, S.E. & Lofgren, S.E. 2013. Does nasal echolocation influence the modularity of the mammal skull? *J. Evol. Biol.* **26** : 2520–2526. Wiley Online Library.

Schnitzler, H.-U., Moss, C.F. & Denzinger, A. 2003. From spatial orientation to food acquisition in echolocating bats. *Trends Ecol. Evol.* **18** : 386–394. Elsevier.

Smith, H.F. 2011. The role of genetic drift in shaping modern human cranial evolution: a test using microevolutionary modeling. *Int. J. Evol. Biol.* **2011** . Hindawi.

Sun, H., Chen, W., Wang, J., Zhang, L., Rossiter, S.J. & Mao, X. 2020. Echolocation call frequency variation in horseshoe bats: molecular basis revealed by comparative transcriptomics. *Proc. R. Soc. B***287** : 20200875. The Royal Society.

Sun, K., Luo, L., Kimball, R.T., Wei, X., Jin, L., Jiang, T., *et al.* 2013. Geographic variation in the acoustic traits of greater horseshoe bats: testing the importance of drift and ecological selection in evolutionary processes. *PLoS One* **8** : e70368. Public Library of Science.

Wagner, G.P. 1996. Homologues, natural kinds and the evolution of modularity. *Am. Zool.* **36** : 36–43. Oxford University Press UK.

Weaver, T.D., Roseman, C.C. & Stringer, C.B. 2007. Were neandertal and modern human cranial differences produced by natural selection or genetic drift? *J. Hum. Evol.* **53** : 135–145. Elsevier.

Westneat, M.W. 2005. Skull biomechanics and suction feeding in fishes.*Fish Physiol.* **23** : 29–75. Elsevier.

Zuri, I., Kaffe, I., Dayan, D. & Terkel, J. 1999. Incisor adaptation to fossorial life in the blind mole-rax Spalax ehrenbergi. *J. Mammal.* **80** : 734–741. American Society of Mammalogists 810 East 10th Street, PO Box 1897, Lawrence˜....